

## Hydrothermal synthesis of nano-size zirconia using commercial zirconia powder: process optimization through response surface methodology

Ashkan Esmaeilifar<sup>1,3</sup>, Soosan Rowshanzamir<sup>1,2\*</sup>, Amin Behbahani<sup>1</sup>

<sup>1</sup>Fuel Cell Laboratory, Green Research Center, Iran University of Science and Technology, Narmak, Tehran, Iran.

<sup>2</sup>School of Chemical Engineering, Iran University of Science and Technology, Narmak, Tehran, 16846-13114, Iran.

<sup>3</sup>National Iranian Gas Company (NIGC), No. 29, South Aban St., Karimkhan Blvd., Tehran, Iran.

### Article Information

Article History:

Received:  
04 January 2015

Accepted:  
26 February 2015

### Keywords

Nano-size zirconia  
Commercial zirconia  
Hydrothermal synthesis  
Response surface methodology.

### Abstract

A hydrothermal method for preparation of nano-size zirconia has been studied to optimize the effective parameters (precursor concentration, temperature and time) using response surface methodology (RSM). The synthesized zirconia samples were characterized through X-ray diffraction (XRD), scanning electron microscope (SEM) and transmission electron microscopy (TEM) analyses to identify mean nanoparticles size of the zirconia powders and molar fraction of monoclinic and tetragonal (or cubic) crystalline phases. Since, tetragonal and cubic phases are more valuable for the technological applications than the monoclinic phase, improving synthesis of tetragonal and cubic crystalline phases has been considered. The analysis of the primary experimental data through RSM method for optimization of the parameters showed that a precursor concentration of about  $0.0092 \text{ mol L}^{-1}$ , a reaction temperature of  $150 \text{ }^\circ\text{C}$  and a reaction time of 83.18 h are the optimum process conditions which give a mean zirconia nanoparticles size of  $\sim 23 \text{ nm}$  and a high molar fraction of tetragonal (or cubic) crystalline phases ( $\sim 70\%$ ) simultaneously.

## 1. Introduction

Zirconia has three thermodynamically stable crystalline phases under atmospheric pressure: monoclinic phase (up to  $1170 \text{ }^\circ\text{C}$ ), tetragonal phase ( $1170\text{--}2370 \text{ }^\circ\text{C}$ ), and cubic phase ( $2370\text{--}2680 \text{ }^\circ\text{C}$ ) [1–5]. Recently, a high-pressure allotropic form of zirconia (orthorhombic) has been reported, this phase is metastable at atmospheric pressure and reverts to the monoclinic phase [1]. Tetragonal and cubic phases

are unstable in pure coarse-grained zirconia at ambient temperature, which is unfortunate because they are more valuable for the technological applications than the monoclinic phase. Consequently, many divalent and trivalent cations (such as  $\text{Mg}^{2+}$ ,  $\text{Ca}^{2+}$ , and rare-earth ions including  $\text{Y}^{3+}$  and  $\text{Sc}^{3+}$ ) have been doped into zirconia to stabilize the metastable cubic and tetragonal phases at room temperature [6]. Zirconia is an important ceramic with a wide range of applications including electrochemical devices,

\*Corresponding author: Tel.: +98 21 77491242; Fax: +98 21 77491242.  
E-mail address: rowshanzamir@iust.ac.ir (S. Rowshanzamir).

structural ceramics, catalytic systems, etc [7].

Cubic phase (CZ), among the three crystalline phases of zirconia, possesses high oxygen ionic conductivity and chemical stability over a wide range of temperature and oxygen partial pressure. Therefore, it is a well-known candidate for applications such as manufacturing of oxygen sensor [5], development of solid oxide fuel cell [8] and catalytic applications (catalyst [9] and catalyst support (such as: Ni/ZrO<sub>2</sub> [10], Co/ZrO<sub>2</sub> [11], Cu/ZrO<sub>2</sub> [12]), promoter [13]) and finally membrane making for separation of oxygen [8]. In other hand, the tetragonal ZrO<sub>2</sub> polycrystal (TZP) ceramics have attracted special attention because of their good mechanical and electrical properties [14] and owing to high oxygen ion conductivity, the high temperature phases (tetragonal and cubic) of ZrO<sub>2</sub> are useful for chemical engineering applications at lower temperatures [15]. Also, the decrease of the grain size below 100 nm leads to the formation of attractive nanostructured ceramics having superior electrical, thermal, optical and mechanical properties [8].

Interest in synthesis and sintering of nano-crystalline ceramics has recently grown due to the significant improvement in their properties as compared to the conventional coarser grain compacts. In order to prepare zirconia nano-crystalline powders, many methods such as

sol-gel, chemical vapor synthesis (CVS), combustion synthesis, precipitation and hydrothermal processing are well known [16,17]. These methods are divided into two groups: liquid phase techniques (usually called wet-chemical synthesis) such as sol-gel or hydrothermal method, and on the other hand, various gas phase processes for examples: inert gas condensation, laser ablation, microwave plasma synthesis and chemical vapor synthesis [18]. The crystalline structures and catalytic properties of zirconia are generally dependent on its synthesis method and thermal treatment [19]. Hydrothermal synthesis refers to the synthesis of a compound in a hydrothermal solution under the effect of temperature >100 °C and pressures above 1 atm. In this method, ceramic sols are produced by chemical reactions in an aqueous or organo-aqueous solution under the

simultaneous application of heat and pressure in the presence of an alkali or acid that has a pseudo-catalytic effect upon the reaction [20]. Hydrothermal process was found most preferable because in this method crystal size can be controlled and miniaturized by altering the process conditions. The reaction such as hydrolysis, co-precipitation, oxidation, decomposition, complexation can be performed using hydrothermal method [17,21]. Hydrothermal synthesis is reported to be a soft chemical route with an important advantage like the formation of phase pure products at low temperature [17,22]. Fig. 1 shows the major differences in the products obtained by conventional techniques and by the hydrothermal method [23].

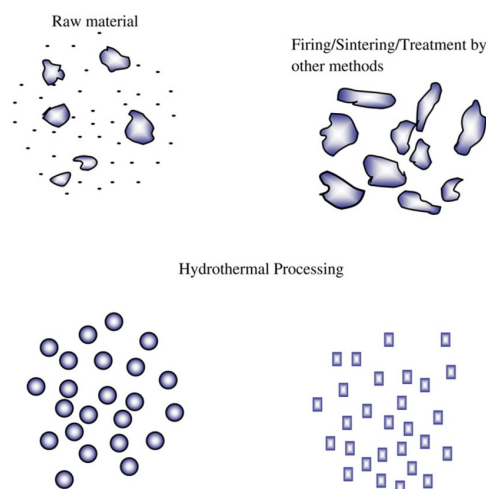


**Fig. 1. Difference in particle processing by hydrothermal and conventional techniques [23].**

In the present work, we investigated a hydrothermal process to synthesis a well controlled nano-size zirconia powder with emphasize on formation of tetragonal or cubic phases of nanoparticles by optimization of the effective operating parameters using response surface methodology (RSM) method. This approach can improve the synthesis of well defined zirconia nanoparticles from commercial zirconia for chemical engineering applications. The structural study of the feed and the products was performed using X-ray diffraction (XRD), scanning electron microscope (SEM) and transmission electron microscope (TEM).

## 2. Experimental

### 2.1. Material and Processing

The starting reagents were commercial zirconia ( $ZrO_2$ , China) and NaOH (Merck, Germany) aqueous solution. The used water in this work was doubly distilled and deionized. At first, a definite amount of the yellow powder, commercial zirconia, was mixed with 75 ml of 10 molar NaOH aqueous solution. The specimen was stirred by a magnetic mixer (Heidolph, MR Hei-Tec) for 3 h with a stirring rate of 850 rpm. Finally, the mixture was transferred into a 100 ml teflon-lined high pressure reactor (BERGHOF, BR-100) and maintained at a specific temperature for a given time.



Fig. 2. The hydrothermal experimental setup.

Temperature regulation was done by means of a temperature probe in a submersion tube to measure the internal reactor temperature which was connected to a temperature controller system (Cole Parmer, Digi-Sense®). The experimental setup is shown in Fig. 2.

### 2.2. Washing, ultrasonic de agglomeration and drying

After hydrothermal treatment of the commercial zirconia, the product which was between sol and gel state (concentrated sol), was obtained. It took around 5–10 h for the whole precipitate to settle down. Subsequently, the product was separated

from the liquid phase by centrifugation (5000 rpm for 5 min).

The semisolid phase was washed several times with dilute HCL (pH = 4–5) and deionized water to remove the hydroxide ions and then dried at 110 °C for 6 h. Afterward, the dried powder was redispersed in acrylonitrile (Merck, Art. 800834) using an ultrasonic device (Sounopuls, Bandelin, HD2200, Germany). Microtip ultrasonication with a frequency of 20 kHz and power of 120 W was used to break up the powder agglomerations in the suspension [14].

### 2.3. Materials Characterization

A Philips PW1800 instrument with Cu  $K\alpha$  radiation was used to obtain the XRD patterns for determination of crystalline phases and particles size of the zirconia powders. The morphology observation and aggregates size distribution was studied using a SEM (TESCAN, VEGA II) and a TEM (Zeiss EM900). Also, X-ray fluorescence (XRF) analysis was performed using a Philips PW1480 instrument in order to determine the composition of commercial zirconia before hydrothermal treatment.

### 2.4. Design of Experiments

In this study, RSM was employed as a tool for systematic experimental design. Experiments using RSM method (design of experiment) allow several effects of factors to be simultaneously determined effectively and efficiently.

RSM, which is a collection of statistical techniques for designing experiments, building models, evaluating the effects of factors and searching for the optimum conditions, has successfully been used in the optimization of processes [24]. This usually leads to an experiment designed to investigate these factors with a view toward eliminating the unimportant ones. This type of experiment is usually called a screening experiment [25]. The most extensive applications of RSM are in the particular situations where several input variables potentially influence some performance measure or quality characteristic of the process. Thus,

performance measure or quality characteristic is called the response. The input variables are sometimes called independent variables, and they are subject to the control of the scientist or engineer [26]. Using the central composite design (CCD) model of RSM method, the optimum level for each factor is determined. CCD has been studied by many statisticians in response surface analysis, and is perhaps the most popular class of second order designs [27]. CCD experiments using RSM was proved to be an optimal tool for optimization of medium parameters for nanoparticles of zirconia production. After the optimum conditions are chosen and predicted, the confirmation experiment should be performed with the prediction.

This confirmation experiment is necessary and important as it provides direct proof of the methodology [23]. In this study, CCD model was employed for design of experiments using RSM, with the three factors (concentration of commercial zirconia in NaOH solution as raw material, temperature and reaction time) and five levels for each one. Description of the employed design of experiments is given in Table 1. The factors and their levels are assigned in Table 2.

**Table 1. Design of experiments using RSM.**

Central Composite Design	Two-level factorial: Full factorial
Factors: 3	Cube points: 8
Replicates: 1	Center points in cube: 4
Base runs: 20	Axial points: 6
Base blocks: 3	Center points in axial: 2
	Alpha: 1.633

**Table 2. Experimental factors and their levels for design of experiment.**

Factor	Level 1	Level 2	Level 3	Level 4	Level 5
concentration of precursor (mol L <sup>-1</sup> )	0.009175	0.025	0.05	0.075	0.090825
Temperature (°C)	110	120	150	180	199
Time (h)	32.8	48	72	96	111.2

Table 3 shows the experimental conditions which are determined by RSM. The initial commercial zirconia concentration in NaOH solution, temperature and reaction time were named as X<sub>1</sub>, X<sub>2</sub> and X<sub>3</sub>, respectively. According to these experimental conditions in Table 3, the influence of factors and optimum experimental conditions will be specified. Minitab software

(Version 14) was used for analysis of the results and process optimization.

**Table 3. Operating conditions of experimental runs.**

Run No.	1	2	3	4	5	6	7	8	9	10
X <sub>1</sub>	0.025	0.075	0.025	0.05	0.05	0.075	0.05	0.05	0.05	0.009175
X <sub>2</sub>	120	120	180	150	150	180	150	150	110	150
X <sub>3</sub>	96	48	48	72	72	96	72	72	72	72
No.	11	12	13	14	15	16	17	18	19	20
X <sub>1</sub>	0.090825	0.05	0.05	0.05	0.075	0.05	0.025	0.025	0.075	0.05
X <sub>2</sub>	150	150	150	199	180	150	120	180	120	150
X <sub>3</sub>	72	111.2	32.8	72	48	72	48	96	96	72

### 3. Result and Discussion

XRF analysis of the commercial zirconia reveals that ZrO<sub>2</sub> (pure zirconia) with 99.45 wt.% is the major component and SiO<sub>2</sub> with 0.11 wt.% is the second one.

#### 3.1. XRD analysis

XRD is of great importance in the microstructure characterization of complex, multiphase and single phase materials. The application of XRD enables not only qualitative and quantitative phase analysis but also microstructure characterization (crystallite size, lattice distortions, dislocation densities, stacking faults and twins probability) [4]. The XRD spectrum of the commercial zirconia is shown in Fig. 3 which reveals the occurrence of monoclinic phase completely. The applied conditions of the twenty experimental runs to prepare hydrothermally synthesized zirconia

nanoparticles are given in Table 3 and the XRD patterns of samples 1, 5, 10 and 15 are shown in Fig. 4 (for example). In these patterns, XRD peaks of cubic or tetragonal phase of nano-crystalline zirconia are observed at  $2\theta = 30.485^\circ$ ,  $35.165^\circ$ ,  $50.644^\circ$ ,  $60.285^\circ$  and  $63.156^\circ$ .

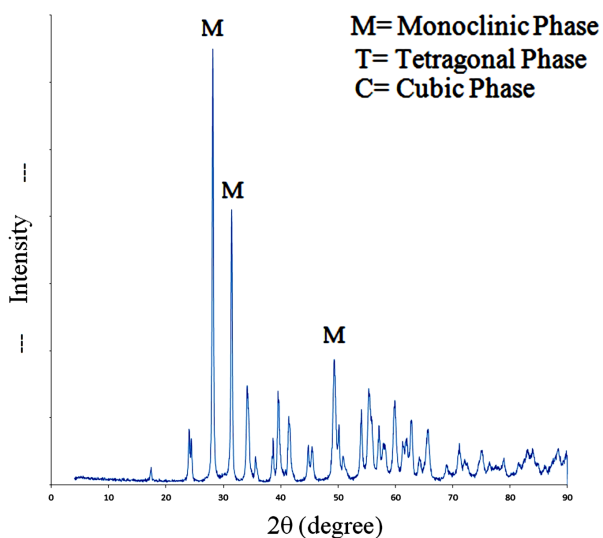


Fig. 3. XRD pattern of the commercial zirconia.

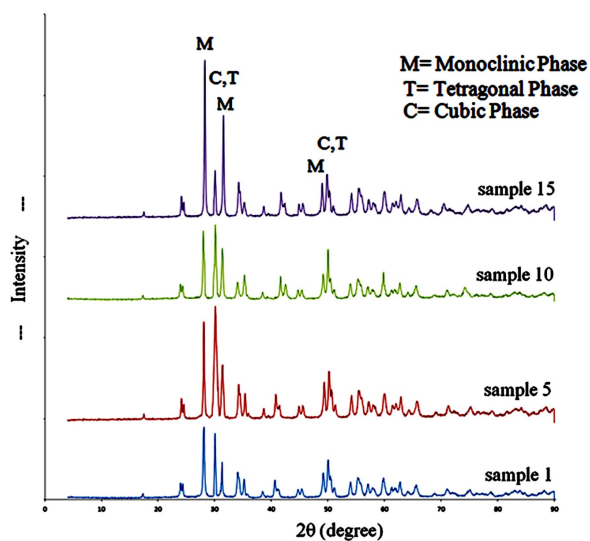


Fig. 4. XRD patterns of the four samples of zirconia nanoparticles synthesized by hydrothermal method.

Therefore, The XRD patterns of the hydrothermally treated zirconia samples (Fig. 4) shows cubic and tetragonal phases in addition to monoclinic phase. The monoclinic and tetragonal crystalline phases can be easily calculated using the difference of their corresponding peaks in the XRD patterns [28]. But, the difference of tetragonal and cubic phases are difficult to determine by XRD patterns, due to their similar lattice parameters and the line broadening of XRD peaks in these patterns [28,29].

The monoclinic, tetragonal and cubic structures were defined with monoclinic, tetragonal and cubic unit cells with the symmetry described by space groups  $P21/c$ ,  $P42/nmc$  and  $Fm3m$ , respectively. The average crystallite sizes after alkali treatment of zirconia in hydrothermal reactor were estimated by the Scherrer equation using the full width at half maximum (FWHM) of the most intense peak ( $2\theta=30.485^\circ$ ). As reported in the literature [23, 28, 30], the Scherrer's equation is described as follows:

$$D = \frac{k * \lambda}{B_{2\theta} * \cos \theta_B} \quad (1)$$

Where  $D$  is the average crystallite size (nm),  $\lambda$  is the X-ray wave length (0.1540593 nm),  $\theta_B$  is the Bragg angle,  $B_{2\theta}$  is the FWHM and  $k=0.9$  is a correction factor to account for particle shapes (a somewhat arbitrary value in range of 0.87–1.0). The intensity data were collected over a  $2\theta$  range of 4–90°. The crystallite sizes of the zirconia prepared by hydrothermal method calculated from the most intense XRD peaks were found to be approximately in the range of 20–50 nm which are given in Table 4. Overall, it shows that hydrothermal treatment of zirconia ( $ZrO_2$ ) by highly concentrated NaOH solution (10 molar) lowers the particles size and increases the content of cubic phase which is very important in chemical engineering applications (e.g. production of catalyst and membrane for solid oxide fuel cells). In cubic phase of zirconia, vacancies increase improves diffusion of oxygen ions as the primary charge carriers which elevates the electrical conductivity [31]. Molar fractions of monoclinic ( $X_m$ ), tetragonal and cubic phases ( $X_{t,c}$ ) of zirconium oxide in product powders were estimated using the equations proposed by Toraya [28]:

$$x_m = \frac{Im(111) + Im(-111)}{Im(111) + Im(-111) + It(101)(orIc(111))} \quad (2)$$

$$x_{t,c} = \frac{It(101)(orIc(111))}{Im(111) + Im(-111) + It(101)(orIc(111))} \quad (3)$$

Where  $Im(111)$  and  $Im(-111)$  are the integral intensities of (111) and (-111) zirconia monoclinic phase peaks (at  $2\theta = 28.037^\circ$ ,  $31.362^\circ$ ), respectively,

and  $I_t(101)$  (or  $I_c(111)$ ) is the integral intensity of (101) (or (111)) tetragonal (or cubic) zirconia phase peak (at  $2\theta = 30.485^\circ$ ). Samples 4, 5, 7, 8, 16 and 20 were synthesized under same experimental conditions, so only sample 4 was reported in Table 4. According to Table 4, the most amounts of cubic or tetragonal crystalline phases (C,T-ZrO<sub>2</sub>) were occurred in samples 1, 10 and 4, respectively.

average size of particles (after an hour dispersing in acrylonitrile) is 0.5 to 3  $\mu\text{m}$ .

Following the hydrothermal treatment, the product was dispersed in acrylonitrile for an hour and then a drop of dispersed liquid was dried on a sample holder for SEM analysis. Fig. 6 shows the SEM images of the alkali treated zirconia in hydrothermal reactor (samples 1, 4 and 10). The SEM photographs of

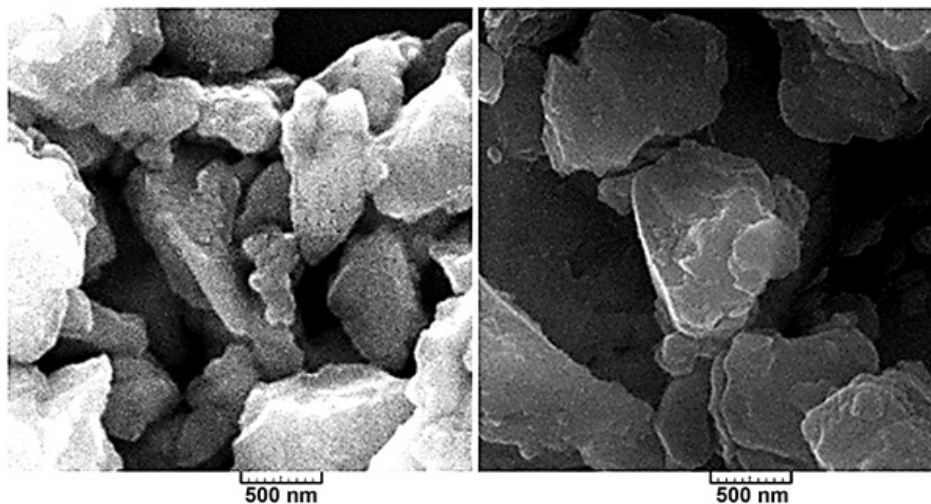
**Table 4. Characterization of the hydrothermally Nano-sized zirconia by XRD analysis.**

Sample	1	2	3	4	6	9	10	11	12	13	14	15	17	18	19
C, T-phases (%)	68	14.45	41.85	55	19.88	35.85	62.95	32.88	39	27.35	33	37	35	37	30
Crystallite size (nm)	20	39	31	30	37	34	27	38	38	36	49	35	34	39	31

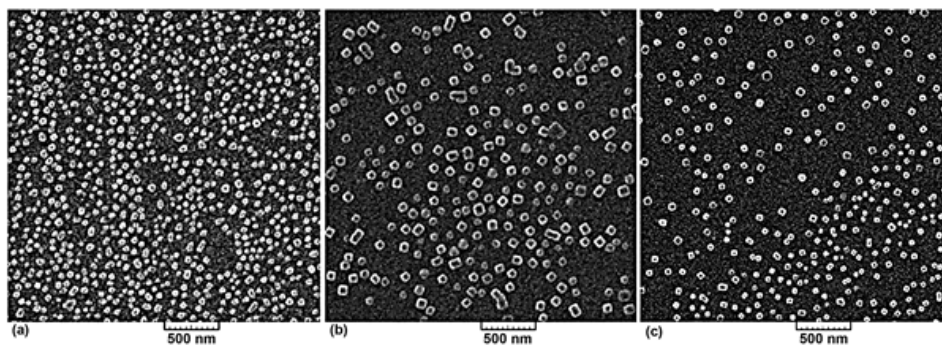
### 3.2. Morphology study

Fig. 5 is the SEM image of the commercial zirconia particles used in this work which shows that the

commercial ZrO<sub>2</sub> (Fig. 5) and the product (Fig. 6) show different morphology. This indicates that hydrothermal treatment of commercial zirconia under alkali condition declines the particles size.



**Fig. 5. SEM micrograph of commercial zirconia before hydrothermal treatment as precursor.**



**Fig. 6. SEM micrographs of nano-size zirconia after hydrothermal treatment ((a) sample 1, (b) sample 4 and (c) sample 10).**

### 3.3. Response surface methodology study

The results of the twenty designed experimental runs are given in Table 4 in the form of synthesized tetragonal (or cubic) crystalline phase percentage (Y) as a response of CCD model. The coefficients of factors and their interactions in the applied model are presented in Table 5. Using Table 5, the CCD model of RSM resulting from the twenty experimental runs under different experimental conditions could be written as following:

$$Y = -398.11 X_1 + 3.18 X_2 + 4.39 X_3 - 4594.64 X_{11} - 0.01 X_{22} - 0.01 X_{33} + 6.10 X_1 * X_2 - 6.19 X_1 * X_3 - 0.01 X_2 * X_3 - 323.87$$

the other factor was kept at level zero [32], e.g. the effect of temperature and reaction time ( $X_2$  and  $X_3$ )

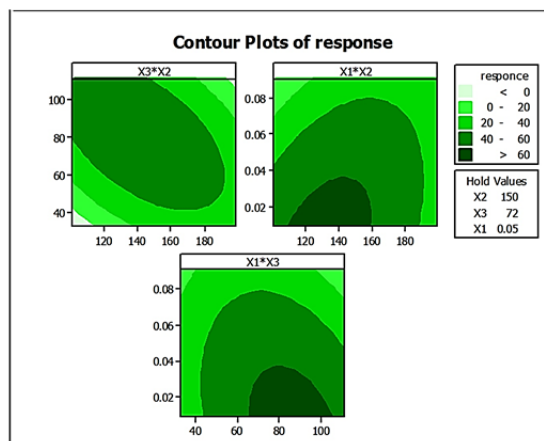


Fig. 8. The contour plots which show the effect of factors and their interactions on response Y.

Table 5. Estimated regression coefficients for response Y.

Factor or interaction	Constant	$X_1$	$X_2$	$X_3$	$X_1 * X_1$	$X_2 * X_2$	$X_3 * X_3$	$X_1 * X_2$	$X_1 * X_3$	$X_2 * X_3$
Estimated effect	-323.87	-398.11	3.18	4.39	-4594.64	-0.01	-0.01	6.10	-6.19	-0.01

The response surfaces model was plotted by using surface and contour plots to study the effects of parameters and their interactions on synthesis of tetragonal and cubic crystalline phases.

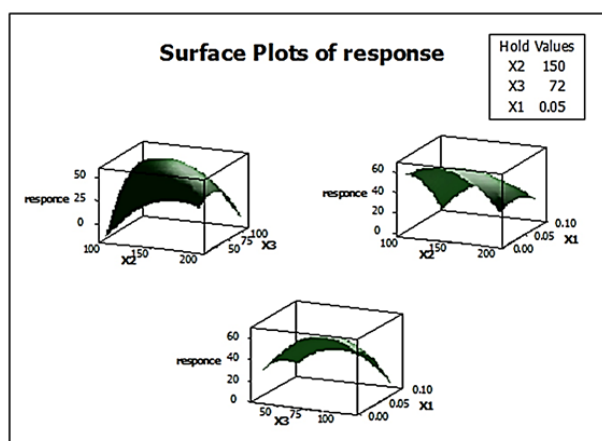


Fig. 7. The response surface plots which show the effect of factors and their interactions on response Y.

Fig. 7 and Fig. 8 show the effect of factors  $X_1$ ,  $X_2$ , and  $X_3$  on the response Y. The three dimensional plots obtained from RSM analysis (surface plot) are displayed in Fig. 7. These types of plots show the effects of two factors on the response at a time while

on the response Y as long as concentration ( $X_1$ ) is at level zero.

The relationship between the factors ( $X_1$ ,  $X_2$  and  $X_3$ ) or independent variables was further elucidated using contour plots which are shown in Fig. 8. Elliptical contours were obtained when there was a perfect interaction between the independent variables [32].

### 3.4. Optimization of the experimental conditions

Response optimization helps to identify the combination of input variable settings that jointly optimize a single response or a set of responses. After generating the polynomial equations relating  $X_1$ ,  $X_2$ , and  $X_3$  factors, the process was optimized for the response Y to obtain the levels of  $X_1$ ,  $X_2$ , and  $X_3$ , which maximized Y. The results of optimization for zirconia nanoparticles in tetragonal or cubic crystalline phase are given in Fig. 9.

According to the given results in Fig. 9, optimum conditions of  $X_1$ ,  $X_2$  and  $X_3$  parameters are 0.0092 mol L<sup>-1</sup>, 150 °C and 83.18 h, respectively. In this case, response optimization by Minitab software predicted that the maximum response under optimum

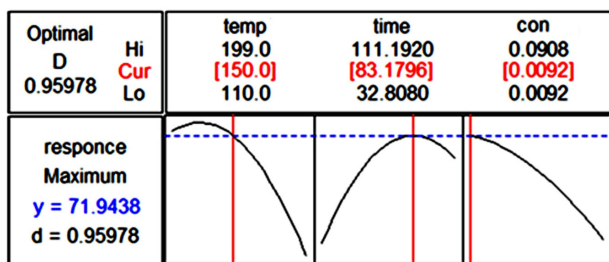


Fig. 9. The results of response optimization.

experimental conditions is nearly 72%. Since the optimum conditions was not equivalent to any of the twenty experimental conditions (Table 3), a sample of zirconia nanoparticles was synthesized under optimum conditions to confirm the predictive result of RSM model (CCD). The XRD spectrum of the optimum zirconia nanoparticles sample is shown in Fig. 10 and the results of XRD analysis are given in Table 6.

Table 6. XRD study of the optimum zirconia nanoparticles sample.

Cubic or Tetragonal phase (%)	Monoclinic phase (%)	Average Crystallite size (nm)
69.85	30.15	22

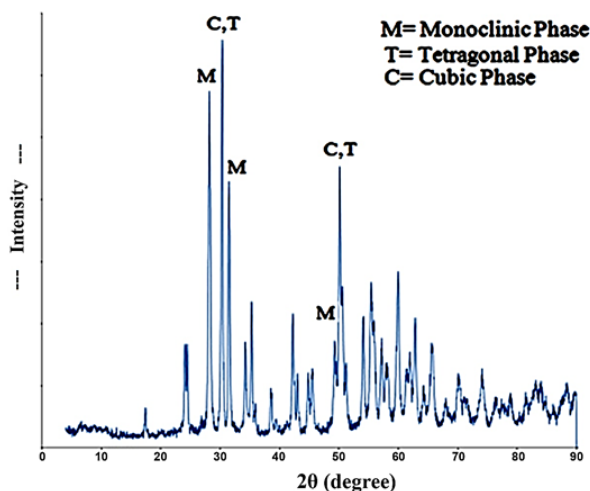


Fig. 10. XRD pattern of the optimum zirconia nanoparticles sample.

According to XRD results, the optimum sample has a 70% of cubic or tetragonal phase of zirconia which confirms the predictive result of the RSM model. The crystalline phase composition of the optimum zirconia nanoparticles sample was calculated by Toraya equations. Also, TEM images (Fig. 11) and the histogram of the optimum zirconia nanoparticles

(Fig. 12(b)) demonstrate that the average size of zirconia nanoparticles is 23.55 nm, which is in accordance with the XRD results (Table 6).

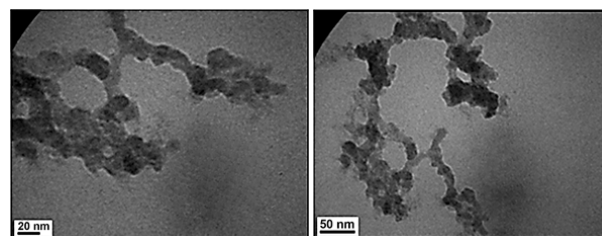


Fig. 11. TEM micrograph of the optimum zirconia nanoparticles sample.

The synthesis parameters affect differently the dispersion and phase composition of ZrO<sub>2</sub>. Despite of the several researches, no exhaustive theory has been developed to predict quantitatively the formation and growth of nano-crystals with a definite crystal structure

as influenced by parameters of a hydrothermal synthesis [33].

Presumably, the decisive factor governing the structure of nano-crystals is the structural similarity of the nucleation centres and growing nano-crystals. This assumption is supported by the fact that the hydroxide of the polymeric hydroxo complex  $[Zr_4(OH)_8 \cdot (H_2O)_{16}]^{8+}$ , which was the ZrO<sub>2</sub> precursor in the hydrothermal synthesis (Fig. 13), has a structure similar to that of cubic (or tetragonal) ZrO<sub>2</sub> [19,33].

When the concentration of oligomers reaches the critical level, crystal nuclei of ZrO<sub>2</sub> are generated and primary particles of ZrO<sub>2</sub> form by growth of these nuclei. Also, when pH of the reaction solution is strongly basic (for example in 10 M solution of NaOH), hydrolysis occurs easily and the concentration of oligomers could reach the critical level and form crystal nuclei [34]. The formation of nanoparticles in the crystalline structure is reported to be associated with the hydroxyl ions inserted in the hydrothermal solution. The mechanism of this process is not completely realized and when the raw material (commercial zirconia) is treated with NaOH in concentrated solution, some of the Zr–O–Zr

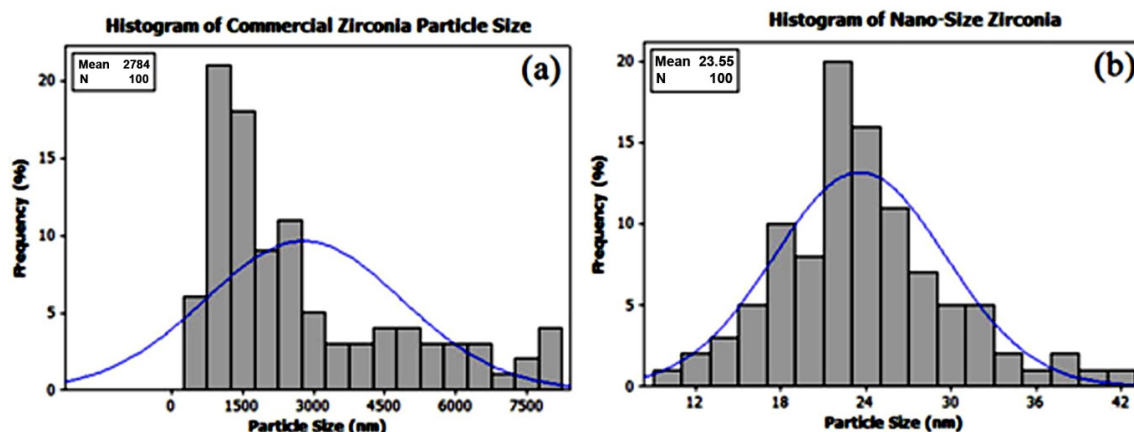


Fig. 12. Particles size histograms of (a) the commercial zirconia and (b) the hydrothermally nano-sized zirconia.

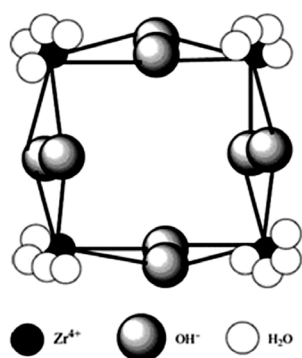


Fig. 13. Schematic of the complex formed from  $ZrO_2$  and NaOH solution [34].

bonds may be broken and then the complexes can form like the one shown in Fig. 13. This complex may change into the nano-size zirconia particles by the hydrothermal treatment.

#### 4. Conclusions

In summary,  $ZrO_2$  nano-powder was successfully obtained by alkali treatment of commercial zirconia powder in a hydrothermal process. For design of experiments with concentration of precursor, reaction temperature and reaction time as effective experimental variables, RSM method was used and the products were characterized through XRF, XRD, SEM and TEM analyses. The XRD results showed that the commercial zirconia crystalline phase was fully monoclinic while after hydrothermal treatment, the

product crystalline phases were cubic and tetragonal phases in addition to monoclinic phase. A highly significant quadratic polynomial including factors and their interactions, obtained by CCD model, was very useful for determining the optimal process parameter values to maximize the molar fraction of cubic or tetragonal phases as response. According to the results of process optimization, a precursor concentration of  $0.0092 \text{ mol L}^{-1}$ , a reaction temperature of  $150 \text{ }^\circ\text{C}$  and a reaction time of 83.18 h were the optimum process conditions which give a cubic (or tetragonal) phase molar fraction of  $\sim 70\%$  and an average particles size of  $\sim 23 \text{ nm}$ .

#### 5. References

- [1] Srinivasan R., De Angelis R. J., Ice G. and Davis B. H., "Identification of tetragonal and cubic structures of zirconia using synchrotron x-radiation source", *J. Mater. Res.*, 1991, 6, 1287.
- [2] Bokhimi X., Morales A., Novaro O., Portilla M., Lopez T., Tzompantzi F. and Gomez R., "Tetragonal Nanophase Stabilization in Nondoped Sol-Gel Zirconia Prepared with Different Hydrolysis Catalysts", *J. Solid State Chem.*, 1998, 135, 28.
- [3] Saylkan F., Asilturk M., Burunkaya E. and Arpac E., "Hydrothermal synthesis and characterization of nanocrystalline  $ZrO_2$  and surface modification with

- 2-acetoacetoxyethyl methacrylate", *J. Sol-Gel Sci. Technol.*, 2009, 51, 182.
- [4] Dercz G., Prusik K. and Pająk L., "Structure investigations of commercial zirconia ceramic powder", *J. Achiev. Mater. Manuf. Eng.*, 2006, 18, 259.
- [5] Nakamura T., Sakamoto Y., Saji K. and Sakata J., "NOX decomposition mechanism on the electrodes of a zirconia-based amperometric NOX sensor", *Sens. Actuators, B*, 2003, 93, 214.
- [6] Xu G., Zhang Y., Liao Ch. and Yan Ch., "Tetragonal-to-Monoclinic Phase Transitions in Nanocrystalline Rare-Earth-Stabilized Zirconia Prepared by a Mild Hydrothermal Method", *J. Am. Ceram. Soc.*, 2004, 87, 2275.
- [7] Chang H., Shady P. and Shih W., "The effects of containers of precursors on the properties of zirconia powders", *Microporous Mesoporous Mater.*, 2003, 59, 29.
- [8] Mazaheri M., Valefi M., Razavi Hesabi Z. and Sadrnezhad S.K., "Two-step sintering of nanocrystalline  $8Y_2O_3$  stabilized  $ZrO_2$  synthesized by glycine nitrate process", *Ceram. Int.*, 2009, 35, 13.
- [9] Su C., Li J., He D., Cheng Z. and Zhu Q., "Synthesis of isobutene from synthesis gas over nanosize zirconia catalysts", *Appl. Catal., A*, 2000, 202, 81.
- [10] Liu Q., Dong X., Mo X. and Lin W., "Selective catalytic methanation of CO in hydrogen-rich gases over Ni/ZrO<sub>2</sub> catalyst", *J. Nat. Gas Chem.*, 2008, 17, 268.
- [11] Panpranot J., Taochaiyaphum N. and Praserttham P., "Glycothermal synthesis of nanocrystalline zirconia and their applications as cobalt catalyst supports", *Mater. Chem. Phys.*, 2005, 94, 207.
- [12] Ma Z. Y., Yang Ch., Wei W., Li W. H. and Sun Y. H., "Catalytic performance of copper supported on zirconia polymorphs for CO hydrogenation", *J. Mol. Catal. A: Chem.*, 2005, 231, 75.
- [13] Therdtianwong S., Siangchin Ch. and Therdtianwong A., "Improvement of coke resistance of Ni/Al<sub>2</sub>O<sub>3</sub> catalyst in CH<sub>4</sub>/CO<sub>2</sub> reforming by ZrO<sub>2</sub> addition", *Fuel Process. Technol.*, 2008, 89, 160.
- [14] Vasylykiv O. and Sakka Y., "Synthesis and Colloidal Processing of Zirconia Nanopowder", *J. Am. Ceram. Soc.*, 2001, 84, 2489.
- [15] Shukla S. and Seal S., "Mechanisms of room temperature metastable tetragonal phase stabilisation in zirconia", *Int. Mater. Rev.*, 2005, 50, 1.
- [16] Widiyastuti W., Balgis R., Iskandar F. and Okuyama K., "Nanoparticle for mationin spray pyrolysis under low-pressure conditions", *Chem. Eng. Sci.*, 2010, 65, 1846.
- [17] Kanade K.G., Baeg J.O., Apte S.K., Prakash T.L. and Kale B.B., "Synthesis and characterization of nanocrystalline zirconia by hydrothermal method", *Mater. Res. Bull.*, 2008, 43, 723.
- [18] Srdic V. V. and Winterer M., "Comparison of nanosized zirconia synthesized by gas and liquid phase methods", *J. Eur. Ceram. Soc.*, 2006, 26, 3145.
- [19] Wang J.A., Valenzuela M.A., Salmenes J., Vázquez A., Garc'ía-Ruiz A. and Bokhimi X., "Comparative study of nanocrystalline zirconia prepared by precipitation and sol-gel methods", *Catal. Today*, 2001, 68, 21.
- [20] Kaya C., He J.Y., Gu X. and Butler E.G., "Nanostructured ceramic powders by hydrothermal synthesis and their applications", *Microporous Mesoporous Mater.*, 2002, 54, 37.
- [21] Miya S.S. and Roy R., "Hydrothermal synthesis of fine oxide powders", *Bull. Mater. Sci.*, 2000, 23, 453.
- [22] Piticescu R., Monty C. and Millers D., "Hydrothermal synthesis of nanostructured zirconia materials: Present state and future prospects", *Sens. Actuators, B*, 2005, 109, 102.

- [23] Esmailifar A., Yazdanpour M., Rowshanzamir S. and Eikani M. H., "Hydrothermal synthesis of Pt/MWCNTs nanocomposite electrocatalysts for proton exchange membrane fuel cell systems", *Int. J. Hydrogen Energy*, 2011, 36, 5500.
- [24] Muthuvelayudham R. and Viruthagiri T., "Application of Central Composite Design Based Response Surface Methodology in Parameter Optimization and on Cellulase Production Using Agricultural Waste", *Int. J. Chem. Biol. Eng.*, 2010, 3, 97.
- [25] Myers R.H., Montgomery D.C. and Anderson C.M., *Response Surface Methodology: Process and Product Optimization Using Designed Experiments*, John Wiley & Sons, 2009.
- [26] Carley K.M., Kamneva N.Y. and Reminga J., *Response Surface Methodology*, CASOS Technical Report, Carnegie Mellon University, 2004.
- [27] Park S.H., Kim H.J. and Cho J.I., *Optimal center composite designs for fitting second order response surface regression models*, Korea Science & Engineering Foundation, 2000.
- [28] Tahmasebpour M., Babaluo A.A. and Aghjeh M.K. R., "Synthesis of zirconia nanopowders from various zirconium salts via polyacrylamide gel method", *J. Eur. Ceram. Soc.*, 2008, 28, 773.
- [29] Ilavsky J. and Stalick J.K., "Phase composition and its changes during annealing of plasma-sprayed YSZ", *Surf. Coat. Technol.*, 2000, 127, 120.
- [30] Szepesi C.J. and Adair J.H., "High Yield Hydrothermal Synthesis of Nano-Scale Zirconia and YTZP", *J. Am. Ceram. Soc.*, 2011, 94, 4239.
- [31] Indarto A., Choi J.W., Lee H. and Song H.K., "A review of C1 chemistry synthesis using yttrium-stabilized zirconia catalyst", *J. Rare Earths*, 2008, 26, 1.
- [32] Yin X., You Q. and Jiang Z., "Optimization assisted extraction of polysaccharides from *Tricholoma matsutake* by response surface methodology", *Carbohydr. Polym.*, 2011, 86, 1358.
- [33] Pozhidaeva O.V., Korytkova E.N., Romanov D.P. and Gusarov V.V., "Formation of ZrO<sub>2</sub> Nanocrystals in Hydrothermal Media of Various Chemical Compositions", *Russ. J. Gen. Chem.*, 2002, 72, 849.
- [34] Qin D. and Chen H., "The influence of alcohol additives on the crystallization of ZrO<sub>2</sub> under hydrothermal conditions", *J. Mater. Sci.*, 2006, 41, 7059.